

Tunable Intramolecular Charge Transfer Effect on Diphenylpyrazine-Based Linear Derivatives and Their Expected Performance in Blue Emitters

Haozhong Wu, Ganggang Li, Juanjuan Luo, Tao Chen, Yao Ma, Zhiming Wang,*
Anjun Qin,* and Ben Zhong Tang

High efficiency deep-blue emitters are one of the basic requests for an outstanding full-color organic light emitting diode (OLED) display. Herein, a linear D-A-D diphenylpyrazine structure is designed for maximizing the π -conjugation effect, whilst two deep-blue (DPP-DPhC and DPP-D3C) and one blue (DPP-DTPA) fluorophores are synthesized by incorporating the *N*-phenylcarbazole and triphenylamine donor units, respectively. As a result, they emit bright deep-blue to blue fluorescence with the luminescence quantum yields of 0.312–0.888 in solid state. Fortunately, all the non-doped and doped OLED devices show deep-blue (*N*-phenylcarbazole disubstituted compounds, DPP-DPhC and DPP-D3C) and blue (triphenylamine derivative, DPP-DTPA) electroluminescence (EL) performance with the maximum external quantum efficiencies (EQEs) of >4%. Comprehensively considering other parameters, the deep-blue non-doped OLED device based on DPP-DPhC exhibits the best EL performance with the maximum EQE of 5.73% with the Commission International de L'Eclairage (CIE_{x,y}) coordinate of (0.151, 0.078) among them. These results demonstrate the feasibility of this strategy and provide a simple method to achieve high efficiency deep-blue emitters.

1. Introduction

Display technologies are the direct way for the smart electronic devices, for example, computers and mobile phones transmitting the message to us. Among many display technologies, organic light-emitting diodes (OLEDs) has been exploring and

developing as its superiorities such as low energy consumption, light weight, large display area and flexibility.^[1] Blue, green, and red three emitters are essential of the full color OLED display. At present, despite these OLED devices have performed satisfactorily and contented the demand of practical applications,^[2–4] high efficiency deep blue emitters with small Commission International de L'Eclairage (CIE_{x,y}) coordinates ($\gamma < 0.10$) are rare and required for wider color gamut on the superior full color OLED displays.^[5]


Generally, electron donating-accepting (D-A) π -conjugated systems are often designed and used in OLED emitters because the molecular structures can be simply modified to adjust the excited states' feature for the specific purpose.^[5b,6] Furthermore, D-A typed structure is seen as the model of bipolar materials that possess good charge mobility. Triphenylamine (TPA) and carbazole are two representa-

tive electron-donating groups and typically as the hole-transport units,^[5b,7,8] while the azacycle structures, for example, pyridine, pyrazine, and triazine are usually as the electron-accepting groups.^[9–11] Inevitably, D-A π -conjugated systems always accompany with intramolecular charge transfer (ICT) characteristic. ICT state possibly causes the redshifted emission which is often the case in green, yellow and red luminophores, but is the adverse factor to construct the blue and deep blue emitting materials.^[12] Therefore, it's very necessary to choose the suitable structures and modulate the ICT effect to achieve high efficiency deep blue emitters.^[5g,13]

Pyrazine derivatives have been explored in the OLED applications because its electron deficiency can be tuned easily via benzo, thieno, etc. modifications.^[14] In deep blue OLEDs, a device fabricated with benzopyrazine-carbazole derivative displayed the maximum external quantum efficiency of 1.20% and CIE coordinates of (0.16,0.07).^[15] Liao and his co-workers designed a twisting carbazole-benzofuro[2,3-*b*]pyrazine emitter whose OLED device achieved the maximum EQE of 4.34% and excellent color purity with CIE_{x,y} (0.15,0.05).^[16] Jiang et al. reported several blue OLED devices with EQEs range from 2.19% to 3.85%.^[17] Our group reported some devices based on tetraphenylpyrazine (TPP) derivatives, but the CIE coordinates did not content the standard of deep blue emission.^[18] When

H. Wu, G. Li, J. Luo, T. Chen, Y. Ma, Z. Wang, A. Qin, B. Z. Tang
AIE institute
State Key Laboratory of Luminescent Materials and Devices
Center for Aggregation-Induced Emission
Guangdong Provincial Key Laboratory of Luminescence
from Molecular Aggregates
Guangzhou International Campus
South China University of Technology (SCUT)
Guangzhou 510640, China
E-mail: wangzhiming@scut.edu.cn; msqinaj@scut.edu.cn

B. Z. Tang
Shenzhen Institute of Aggregate Science and Technology
School of Science and Engineering
The Chinese University of Hong Kong
Shenzhen, Guangdong 518172, China

 The ORCID identification number(s) for the author(s) of this article can be found under <https://doi.org/10.1002/adom.202101085>.

DOI: 10.1002/adom.202101085

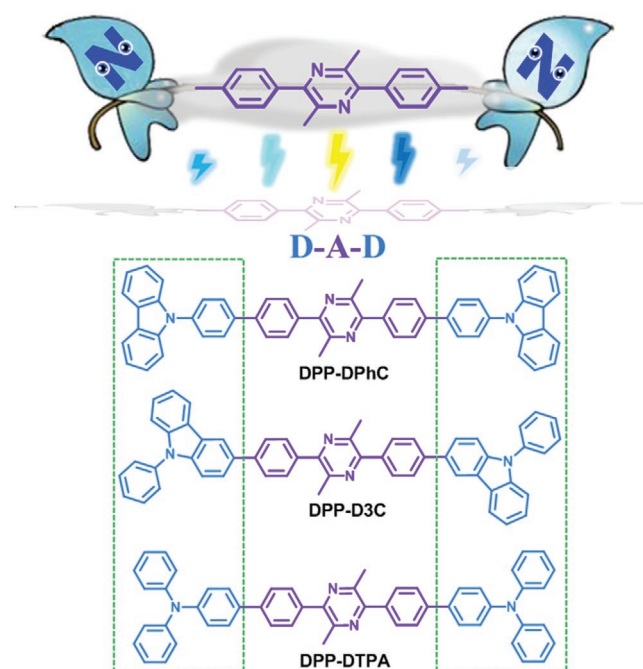


Figure 1. The molecular design of deep-blue emitters and the structures of the three DPP derivatives.

the *ortho* phenyl group replacing by a methyl group on TPP, the deep blue EL emission with EQE of 2.89% could be achieved.^[19] Nevertheless, the high efficiency deep blue OLEDs based on pyrazine structures still has much development potential.

Recently, our group figured out the structure-property relationship of TPP compounds that *ortho*-substitution can distort the molecular structure and prevent the serious π - π stacking while the substitution on *para*-position can significantly enhance the luminescence.^[20] Besides, the replacement of phenyl group by methyl group can blueshift its emission.^[19] Considering that, the linear D-A-D pyrazine structure was designed to maximize the *para*-substitution effect while two methyl groups on *ortho*-position of pyrazine was expected to avoid the intermolecular stacking between pyrazine center (A) and D units.^[21] Follow this strategy, classical blue fluorophores *N*-phenylcarbazole and triphenylamine were chosen to construct three deep blue and blue luminescent molecules, namely DPP-DPhC, DPP-D3C, and DPP-DTPA (Figure 1). Photophysical properties, single crystal structures and theoretical calculation reveal that the donors influence the electron-hole distribution and the luminescence process can be simply tuned by their electron-donating ability. Consequently,

all the doped and non-doped fabricated with three diphenylpyrazine (DPP) derivatives exhibit deep blue to blue electroluminescence (EL) emission with the peaks at 406–462 nm and >4% maximum EQE. In particular, the non-doped device based on DPP-DPhC shows the excellent deep blue OLED performance with the maximum EQE and CIE coordinate of 5.73% and (0.151, 0.078), respectively. This contribution offers a feasible approach for developing high performance deep blue emitters.

2. Results and Discussion

2.1. Synthesis and Characterization

The synthetic route of the three target products was outlined in Figure S1, Supporting Information. Detail synthesis process and characterization were provided in the Supporting Information (Figures S2–S11, Supporting Information). 1-(4-bromophenyl)-2-hydroxypropan-1-one was prepared according to the reported literature^[19] and it transformed to DPP-2Br under the ammonium acetate and cerous chloride heptahydrate condition. DPP-DPhC, DPP-D3C, and DPP-DTPA were obtained from DPP-2Br and corresponding boronic acid derivatives via Suzuki coupling reaction. Good thermal stability and morphological stability are the basic requirement of OLED emitters, so the three DPP derivatives were tested by thermogravimetric analysis and differential scanning calorimetry. They possess the excellent thermal stability with the temperatures of 5% weight loss (T_d) as high as 472, 501, and 478 °C respective for DPP-DPhC, DPP-D3C, and DPP-DTPA (listed in Table 1). Besides, DPP-D3C and DPP-DTPA show the good morphological stability with glass transition temperatures (T_g) of 129 and 108 °C, while DPP-DPhC does not transform into another phase in wide temperature range (Figure S12, Supporting Information).

2.2. Photophysical Properties

Photophysical properties of the DPP compounds were analyzed based on the absorption spectra and photoluminescence (PL) spectra. As shown in Figure 2A, three DPP derivatives exhibit the analogous absorption profile. DPP-DPhC shows the absorptive band of 300–380 nm with the peak at 341 nm in tetrahydrofuran (THF) solution, referred to the π - π transition of whole skeleton, while the absorptive bands (peaks) of DPP-D3C and DPP-DTPA redshift to 310–400 nm (341 nm) and 320–430 nm (360 nm) accompanying with larger absorptivity, respectively,

Table 1. The photophysical property of three DPP compounds.

Compound	$\lambda_{\text{abs}}^{\text{a}}$ [nm]	$\lambda_{\text{em}}^{\text{b}}$ [nm]		Φ^{c}		τ^{d} [ns]		T_d^{e} [°C]	T_g^{f} [°C]
		THF	solid	THF	solid	THF	solid		
DPP-DPhC	341	426	415	0.258	0.312	0.59	1.05	472	–
DPP-D3C	342	436	439	0.483	0.888	0.71	1.12	501	129
DPP-DTPA	360	472	464	0.861	0.708	1.63	1.32	478	108

^a)maximum absorption wavelength, concentration: 10^{-5} M; ^b)maximum emission wavelength; ^c)absolute fluorescence quantum efficiency; ^d)fluorescence lifetime; ^e)temperature of 5% weight loss; ^f)glass transition temperatures.

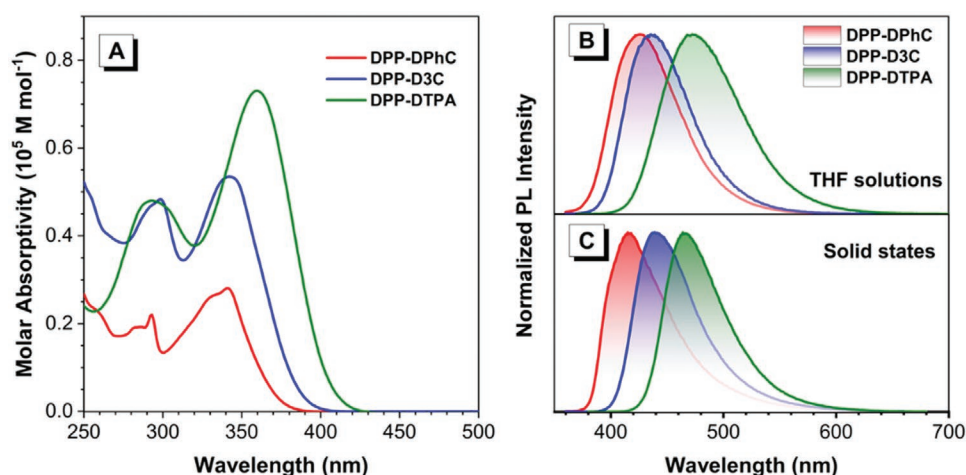


Figure 2. A) The absorption spectra of three compounds in THF solutions (10^{-5} M). The PL spectra of three compounds in B) THF solutions (10^{-5} M) and C) solid states.

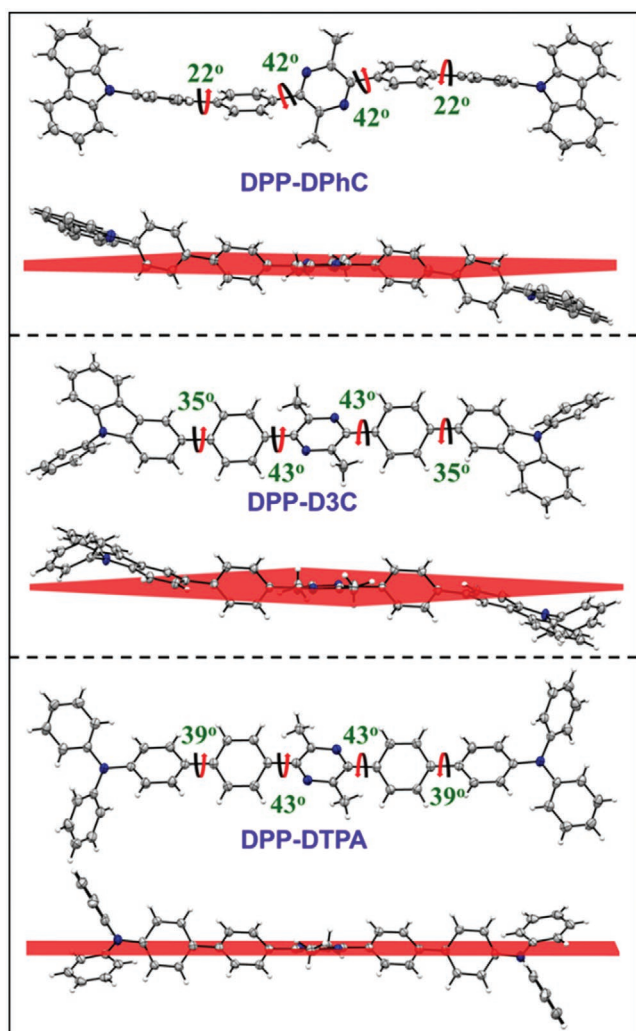


Figure 3. The molecular structures of the three DPP derivatives in single crystals.

due to the stronger donating nature of D units and their larger π -conjugation. Under excitation of UV lamp, DPP-DPhC shows deep blue luminescence with the emission peak (λ_{em}) of 426 nm and the absolute fluorescence quantum efficiency (Φ) of 0.258 in THF solution, when the λ_{em} of DPP-D3C and DPP-DTPA respectively shift to 436 and 472 nm as well as their Φ s are up to 0.483 and 0.861 in THF solutions (Figure 2B and Table 1). The redshifted and efficient PL emission is attributed to the stronger ICT effect caused by the difference of donors (ICT effect were measured and analyzed in Figure S13 and Table S1, Supporting Information). Besides, the lifetimes with 0.5–1.8 ns demonstrates their ordinary fluorescence nature (Figure S14, Supporting Information). As expected, three DPP derivatives emit bright deep blue to blue fluorescence with Φ s of 0.312–0.888 in solid states, strongly suggesting the feasibility of our strategy on high efficiency emitters.

2.3. Single Crystal Structure

The single crystals of three DPP derivatives were achieved by the evaporation from dichloromethane solution or n-hexane/dichloromethane mixtures. Detailed analysis of the resulting X-ray diffraction (XRD) data were shown in supporting information (Table S2 and Figures S15, S16, Supporting Information). As shown in Figure 3, the twisting angles between pyrazine center and phenyl bridge are 42–43° in three DPP compounds, whilst the π -D angles increase in the order of the electron-donating ability of D units (22° for DPP-DPhC, 35° for DPP-D3C and 39° for DPP-DTPA). It's worth mentioning that some bending among D units and π -A- π moiety was observed in the carbazole-substituted compounds DPP-DPhC and DPP-D3C. From the perspective of packing situation (Figure S15, Supporting Information), no π - π stacking happen on the DPP-DPhC and DPP-DTPA, but only carbazole to carbazole π - π interactions with the distance of 3.379 and 3.526 Å exist in the DPP-D3C crystal. It seems that the π - π stacking among D units will not undermine the luminescence efficiency, but can cause the redshift of fluorescence (Table 1). Usually, the

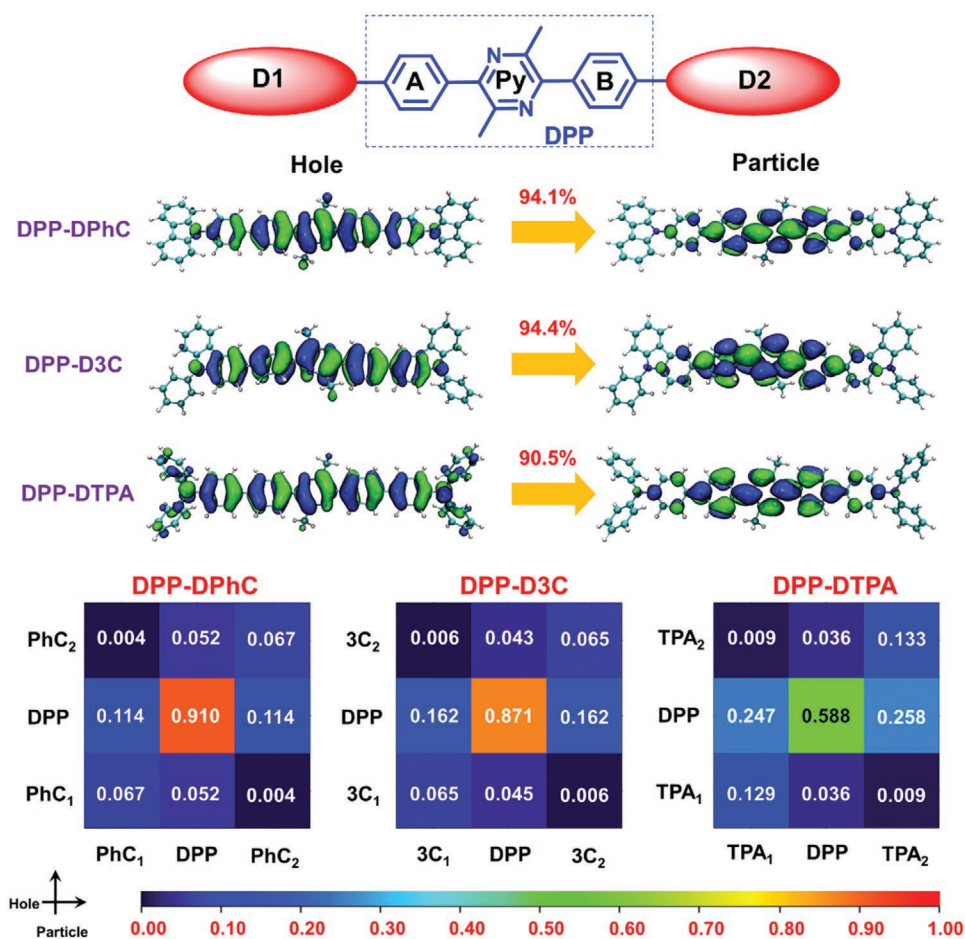


Figure 4. The NTO distribution (isovalue = 0.02) and transition density matrices of the three compounds in S_1 states.

strong and more C-H $\cdots\pi$ intermolecular interactions can afford a rigid environment and block the molecular motions. As illustrated in Figure S16, Supporting Information, DPP-DPhC only has two C-H $\cdots\pi$ interactions with the relatively long distance of 3.016 Å, however, four C-H $\cdots\pi$ interactions (2.707–2.987 Å) and six C-H $\cdots\pi$ interactions (2.843–3.091 Å) were shown in DPP-D3C and DPP-DTPA crystal, respectively, thus their rigid environment is partly responsible for the high Φ_s of DPP-D3C and DPP-DTPA in solid states.

2.4. Theoretical Calculation

To get deep insight the disparity of three DPP compounds, their geometries of ground states (S_0) and the first singlet excited states (S_1) were optimized at M06-2X/6-31G (d,p) level with the polarizable continuum model of THF solvent in Gaussian 16 package. In S_0 states, three DPP derivatives are the relatively twisted structures that the pyrazine centers, phenyl bridges and D units all show the distorted angle of 36–40°, while their two substituted arms bend with only 6–7°; Interestingly, the torsion angles among pyrazine, phenyl bridges and D units decrease but the bending angles of two arms increase for three DPP compounds in S_1 states with respect to these in

S_0 states (Figure S17 and Table S3, Supporting Information). The large geometrical change is commonly restricted in solid states, which is the main reason for the blue-shifted emission of DPP-DPhC and DPP-DTPA in solid states comparing to their THF solutions.^[22] For DPP-D3C, although this restriction can be activated in solid state, its carbazole to carbazole stacking effect overwhelms the former effect and results in its slightly redshifted PL spectrum in solid states. To understand their S_1 transition nature, natural transition orbitals (NTO) based on their S_1 geometries were performed and shown in Figure 4. Both holes and particles are almost dispersed on the pyrazine center, phenyl bridges and phenyl groups of D units for three DPP compounds, implying for the relatively obvious electron-hole overlap. The transition density matrices of S_1 state were analyzed in the multiwfn program.^[23] In the matrix, the value of each block (noted {X, Y}) represents the transition density of the hole on X unit transiting to the particle on Y unit. Obviously, the blocks {DPP, DPP} of three compounds possess the maximum transition densities, suggesting that their transition of S_1 states are mainly related to DPP units, especially for DPP-DPhC. Comparing to DPP-DPhC, altering the connection mode of *N*-phenylcarbazole can increase its conjugation effect, which results in an increase contribution of the D units and slight decrease contribution of DPP unit to the S_1 transition.

Table 2. The EL performance of these non-doped and doped devices.

Emitter Layers	λ_{EL} [nm]	$V_{\text{on}}^{\text{a)}}$ [V]	$L^{\text{b)}}$ [cd m ⁻²]	$\eta_{\text{c}}^{\text{b)}}$ [cd A ⁻¹]	$\eta_{\text{p}}^{\text{b)}}$ [lm W ⁻¹]	EQE _{max} /EQE @ 1000 cd m ⁻² [%]	RO ^{c)} [%]	CIE ^{d)} (x, y)
DPP-DPhC	424	3.6	2741	3.12	2.23	5.73/4.51	21	(0.151, 0.078)
DPP-D3C	434	3.2	7905	3.13	2.88	4.68/4.54	3	(0.149, 0.093)
DPP-DTPA	454	3.0	12 903	4.93	5.16	4.13/3.87	6	(0.145, 0.166)
CBP: DPP-DPhC	406	3.6	2058	1.87	1.47	5.53/3.78	32	(0.157, 0.061)
mCP: DPP-DPhC	404	3.6	2653	2.14	1.84	5.80/3.83	34	(0.167, 0.084)
DPEPO: DPP-DPhC	418	3.6	783	1.74	1.30	4.66/-	100	(0.153, 0.066)
CBP: DPP-D3C	420	3.4	3412	2.28	1.83	5.13/4.78	7	(0.152, 0.071)
mCP: DPP-D3C	420	3.4	2783	2.08	1.59	4.91/4.47	9	(0.153, 0.070)
DPEPO: DPP-D3C	428	3.6	792	3.01	2.36	5.33/-	100	(0.150, 0.084)
CBP: DPP-DTPA	450	3.0	7200	5.27	4.79	5.15/4.60	11	(0.146, 0.138)
mCP: DPP-DTPA	450	3.2	7371	4.07	3.45	4.05/3.70	9	(0.147, 0.135)
DPEPO: DPP-DTPA	462	3.2	2642	7.46	6.89	5.81/3.55	39	(0.147, 0.184)

^{a)} V_{on} is the turn-on voltage at 1 cd m⁻²; ^{b)} The luminance (L), current efficiency (η_{c}) and power efficiency (η_{p}) are the maximum values of the devices; ^{c)} roll-off on EQE; ^{d)} CIE coordinates at 10 mA cm⁻².

For example, {3C₁, DPP} and {3C₂, DPP} of DPP-D3C show the increase transition densities, while its {DPP, DPP} transition density decreases, against to DPP-DPhC. For triphenylamine-disubstituted derivative, despite the highest density value still on {DPP, DPP} block, it decreases remarkably, whilst the transition densities relative to TPA ({TPA₁, DPP}, {TPA₂, DPP}, {TPA₁, TPA₁}, and {TPA₂, TPA₂}) increase significantly. These analyses indicate that the introduction of strong D units can delocalize the S₁ transition distribution more on the whole molecules and enhance the ICT strength. Meanwhile, the oscillator strength (f) increment in the order of DPP-DPhC (2.5603), DPP-D3C (2.6672), and DPP-DTPA (2.8415) demonstrates the modification with strong D units is benefit to S₁ radiative transition process again. Therefore, the strong D units such as TPA can significantly reduce the DPP involvement on the S₁ radiation and enlarge the conjugation, which facilitates the intense fluorescence in DPP-DTPA. However, the enhanced ICT characteristic due to the strong electron-donating substitution will also cause the redshifted λ_{em} of DPP-DTPA which is detrimental to achieve deep blue emitters, thus DPP-DTPA can merely serve as the blue emitting materials.

2.5. Electroluminescence Performance

As the efficient deep blue and blue emission of DPP-DPhC, DPP-D3C, and DPP-DTPA, we evaluated their electroluminescence (EL) performance. First, the HOMO/LUMO levels were approximatively acquired and showed in Figure S18 and Table S4, Supporting Information. After that, the non-doped devices were fabricated with the configuration of ITO/HATCN (5 nm)/TAPC (40 nm)/TCTA (5 nm)/EML (20 nm)/TPBi (40 nm)/LiF (1 nm)/Al (120 nm), in which HATCN ((2,3,6,7,10,11-hexacyano-1,4,5,8,9,12-hexaazatriphenylene)) and TAPC (1,1-bis(4-di-p-tolylaminophenyl)cyclohexane) serve

as the hole-injecting layer and hole-transporting layer, respectively. TCTA (4,4',4''-tri-9-carbazolytriphenylamine) acts as the hole-transporting layer and electron-blocking layer, and TPBi (2,2',2''-(1,3,5-benzinetriyl)tris(1-phenyl-1-H-benzimidazole)) are used as the electron-transporting layer and hole-blocking layer. The key data and characteristic curves are given in **Table 2** and **Figure 5**. The turn-on voltage of non-doped devices increase in order of DPP-DTPA, DPP-D3C, and DPP-DPhC, which is consistent to their energy gap. Expectedly, the non-doped device based on DPP-DPhC displays the deep blue EL emission with the maximum EQE up to 5.73% and CIE coordinate of (0.151, 0.078). Similarly, the non-doped device based on DPP-D3C also shows the deep blue EL performance with the maximum EQE of 4.68% and CIE coordinate of (0.149, 0.093). To DPP-DTPA, its non-doped device exhibits the blue emission with the maximum EQE of 4.13% and CIE_{x,y} (0.145, 0.166). To achieve the higher efficiency EL performance, the 4,4'-bis(*N*-carbazolyl)-1,1'-biphenyl (CBP), 1,3-bis(carbazol-9-yl)benzene (mCP) and bis[2-(diphenylphosphino)phenyl]ether oxidethe (DPEPO) were chosen as the host materials and the doped devices with the structure of ITO/HATCN (5 nm)/TAPC (50 nm)/TCTA (5 nm)/host:10 wt%guest (20 nm)/TPBi (40 nm)/LiF (1 nm)/Al (120 nm) were prepared (curves are listed in Figures S19–S21, Supporting Information).

As shown in Table 2, the turn-on voltages of doped devices are almost higher than that of their respective non-doped devices and the EL peaks (λ_{EL}) nearly shift to the bluer region. For DPP-DPhC, doping in the mCP host material can only slightly increase the EQE to 5.80%, but with the scarification of the color purity, while the contrary circumstance happened on doping in CBP and DPEPO host materials (Figure 5F and Figure S19). Comparing to DPP-DPhC, doping fabrication on DPP-D3C with three chosen host materials can concurrently improve the EQE and decrease the CIE_p. Among the DPP-D3C devices, the device based on DPEPO:DPP-D3C shows the

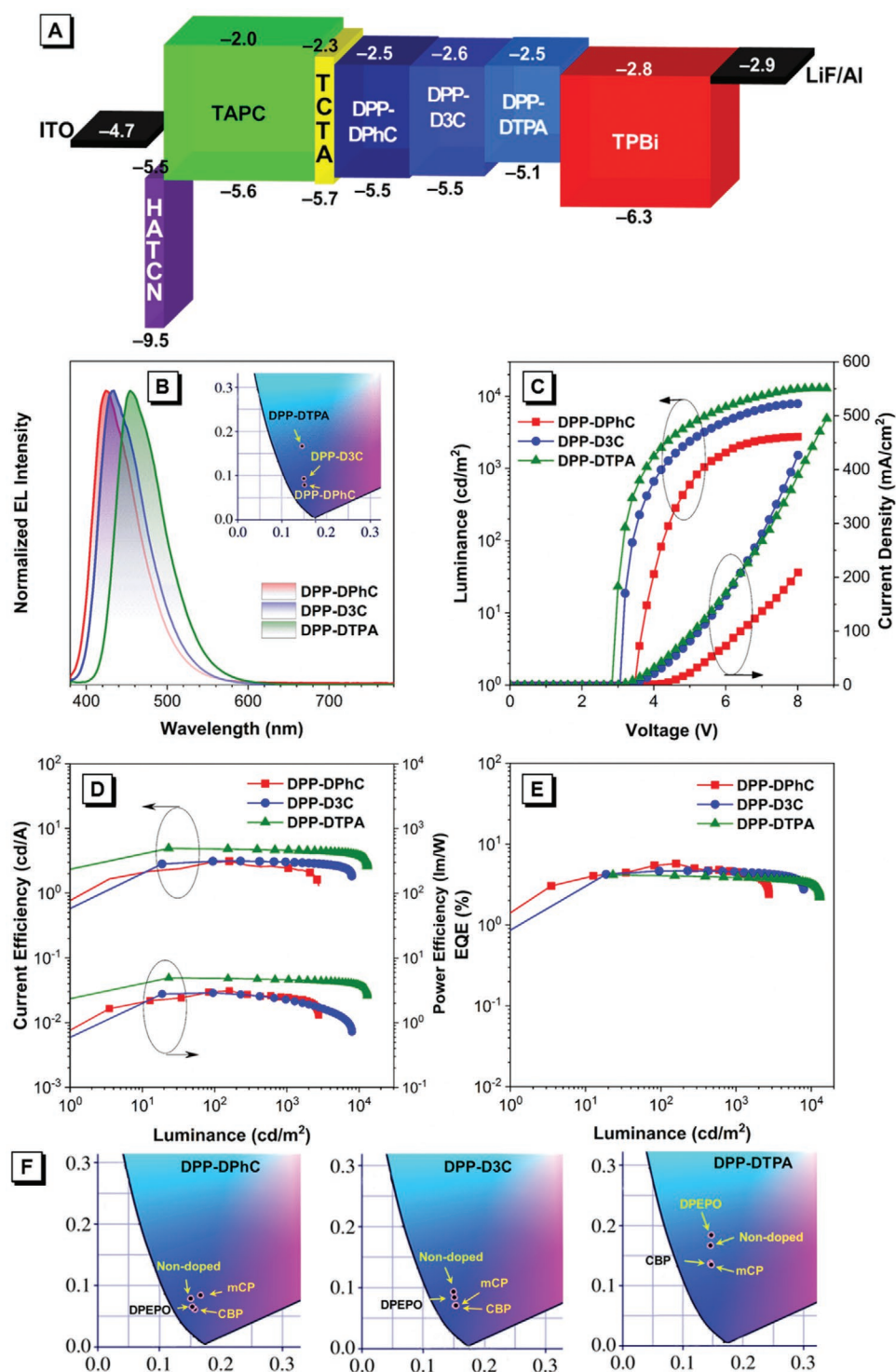


Figure 5. A) The device configuration. B) EL spectra, C) current density–voltage–luminance, D) current efficiency–luminance–power efficiency, and E) EQE–luminance curves of three non-doped devices. F) The CIE coordinates of all the OLED devices.

highest EQE of 5.33% with the CIE_{x,y} (0.150, 0.084) (Figure S20, Supporting Information). For DPP-DTPA, the polar host DPEPO can elevate the maximum EQE to 5.81%, but cause the unexpected redshift (Figure S21, Supporting Information). It must be mentioned that the doped devices exhibit large roll-off

on EQEs, especially in the DPEPO host material. Comprehensively considering all the parameters, non-doped OLED fabrication can furnish the excellent EL performance for DPP-DPhC, when selecting CBP as host is the optimum scheme for both DPP-D3C and DPP-DTPA. In all these devices, the non-doped

device of DPP-DPhC displays the best deep blue OLED performances.

3. Conclusion

Two deep blue emitters (DPP-DPhC and DPP-D3C) and a blue emitter (DPP-DTPA) with the linear D- π -A- π -D mode were designed. In solutions, the fluorescence gradually increases from DPP-DPhC, DPP-D3C to DPP-DTPA because modifying with strong D units can reduce the contribution of electron-deficient pyrazine on S_1 state and expand the delocalization. In solid states, no deleterious π - π packing exists, which can provide them with good luminescence. As expected, the nondoped device based on DPP-DPhC achieves the best deep blue EL emission with the maximum EQE of 5.70% and the CIE coordinate of (0.151, 0.078). By the means of doping, the maximum EQE up to 5% of DPP-D3C and DPP-DTPA based devices can be easily attained. This work introduces a simple and effective avenue for developing deep blue emitters and it's anticipated that the high efficiency violet-blue emitters with small CIE_y can be realized in the V-shaped structure or *meta*-connection.

Supporting Information

Supporting Information is available from the Wiley Online Library or from the author.

Acknowledgements

H. Wu and G. Li contributed equally to this work. The authors are grateful for financial support from the National Natural Science Foundation of China (21788102 and 21975077), National Key R&D Program of China (Intergovernmental cooperation project, 2017YFE0132200), Open Research Project of Military Logistics Support Department (BLB19J008), the Fundamental Research Funds for the Central Universities (2019ZD04), Natural Science Foundation of Guangdong Province (2020A1515011542) and Fund of Guangdong Provincial Key Laboratory of Luminescence from Molecular Aggregates (2019B030301003).

Conflict of Interest

The authors declare no conflict of interest.

Data Availability Statement

The data that supports the findings of this study are available in the supplementary material of this article.

Keywords

charge transfer, deep-blue emission, diphenylpyrazine, high efficiency, organic light-emitting diodes

Received: May 31, 2021
Revised: July 14, 2021
Published online:

- [1] a) C. W. Tang, S. A. Vanslyke, C. H. Chen, *J. Appl. Phys.* **1989**, *65*, 3610; b) L. Xiao, Z. Chen, B. Qu, J. Luo, S. Kong, Q. Gong, J. Kido, *Adv. Mater.* **2011**, *23*, 926; c) S. Scholz, D. Kondakov, B. Lüssem, K. Leo, *Chem. Rev.* **2015**, *115*, 8449; d) M. Yu, R. Huang, J. Guo, Z. Zhao, B. Z. Tang, *Photonix* **2020**, *1*, 11. e) J. Yang, Z. Chi, W. Zhu, B. Z. Tang, Z. Li, *Sci. China Chem.* **2019**, *62*, 1090.
- [2] a) T. Hatakeyama, K. Shiren, K. Nakajima, S. Nomura, S. Nakatsuka, K. Kinoshita, J. Ni, Y. Ono, T. Ikuta, *Adv. Mater.* **2016**, *28*, 2777; b) X. Liang, Z.-P. Yan, H.-B. Han, Z.-G. Wu, Y.-X. Zheng, H. Meng, J.-L. Zuo, W. Huang, *Angew. Chem. Int. Ed.* **2018**, *57*, 11316; c) B. Chen, B. Liu, J. Zeng, H. Nie, Y. Xiong, J. Zou, H. Ning, Z. Wang, Z. Zhao, B. Z. Tang, *Adv. Funct. Mater.* **2018**, *28*, 1803369; d) X. Tang, Q. Bai, T. Shan, J. Li, Y. Gao, F. Liu, H. Liu, Q. Peng, B. Yang, F. Li, P. Lu, *Adv. Funct. Mater.* **2018**, *28*, 1705813; e) F. Liu, H. Liu, X. Tang, S. Ren, X. He, J. Li, C. Du, Z. Feng, P. Lu, *Nano Energy* **2020**, *68*, 104325; f) H. Zhang, B. Zhang, Y. Zhang, Z. Xu, H. Wu, P.-A. Yin, Z. Wang, Z. Zhao, D. Ma, B. Z. Tang, *Adv. Funct. Mater.* **2020**, *30*, 2002323.
- [3] a) Y. Seino, S. Inomata, H. Sasabe, Y.-J. Pu, J. Kido, *Adv. Mater.* **2016**, *28*, 2638; b) T.-L. Wu, M.-J. Huang, C.-C. Lin, P.-Y. Huang, T.-Y. Chou, R.-W. Chen-Cheng, H.-W. Lin, R.-S. Liu, C.-H. Cheng, *Nat. Photonics* **2018**, *12*, 235; c) J. Guo, Z. Zhao, B. Z. Tang, *Adv. Optical Mater.* **2018**, *6*, 1800264; d) Q. Wei, N. Fei, A. Islam, T. Lei, L. Hong, R. Peng, X. Fan, L. Chen, P. Gao, Z. Ge, *Adv. Optical Mater.* **2018**, *6*, 1800512; e) D. Zhang, X. Song, M. Cai, H. Kaji, L. Duan, *Adv. Mater.* **2018**, *30*, 1705406; f) Y. Xu, Z. Cheng, Z. Li, B. Liang, J. Wang, J. Wei, Z. Zhang, Y. Wang, *Adv. Optical Mater.* **2020**, *8*, 1902142.
- [4] a) H. Wang, L. Meng, X. Shen, X. Wei, X. Zheng, X. Lv, Y. Yi, Y. Wang, P. Wang, *Adv. Mater.* **2015**, *27*, 4041; b) J. H. Kim, J. H. Yun, J. Y. Lee, *Adv. Optical Mater.* **2018**, *6*, 1800255; c) J. Liang, C. Li, Y. Cui, Z. Li, J. Wang, Y. Wang, *J. Mater. Chem. C* **2020**, *8*, 1614; d) H. Yu, X. Song, N. Xie, J. Wang, C. Li, Y. Wang, *Adv. Funct. Mater.* **2021**, *31*, 2007511.
- [5] a) R. Chavez, III, M. Cai, B. Tlach, D. L. Wheeler, R. Kaudal, A. Tsyrenova, A. L. Tomlinson, R. Shinar, J. Shinar, M. Jeffries-EL, *J. Mater. Chem. C* **2016**, *4*, 3765; b) S.-J. Woo, Y. Kim, M.-J. Kim, J. Y. Baek, S.-K. Kwon, Y.-H. Kim, J.-J. Kim, *Chem. Mater.* **2018**, *30*, 857; c) J. Yang, Q. Guo, J. Wang, Z. Ren, J. Chen, Q. Peng, D. Ma, Z. Li, *Adv. Optical Mater.* **2018**, *6*, 1800342; d) L. Peng, J.-W. Yao, M. Wang, L.-Y. Wang, X.-L. Huang, X.-F. Wei, D.-G. Ma, Y. Cao, X.-H. Zhu, *Sci. Bull.* **2019**, *64*, 774; e) H. Lim, H. J. Cheon, S.-J. Woo, S.-K. Kwon, Y.-H. Kim, J. J. Kim, *Adv. Mater.* **2020**, *32*, 2004083; f) S. Ye, Y. Wang, R. Guo, Q. Zhang, X. Lv, Y. Duan, P. Leng, S. Sun, L. Wang, *Chem. Eng. J.* **2020**, *393*, 124694; g) Z. Shen, X. Zhu, W. Tang, X. J. Feng, Z. Zhao, H. Lu, *J. Mater. Chem. C* **2020**, *8*, 9401.
- [6] a) X. Cai, S.-J. Su, *Adv. Funct. Mater.* **2018**, *28*, 1802558; b) L. Yu, Z. Wu, G. Xie, W. Zeng, D. Ma, C. Yang, *Chem. Sci.* **2018**, *9*, 1385. c) H. J. Kim, M. Godumala, S. K. Kim, J. Yoon, C. Y. Kim, H. Park, J. H. Kwon, M. J. Cho, D. H. Choi, *Adv. Optical Mater.* **2020**, *8*, 1902175; d) G. Li, F. Zhan, W. Lou, D. Wang, C. Deng, L. Cao, Y. Yang, Q. Zhang, Y. She, *J. Mater. Chem. C* **2020**, *8*, 17464.
- [7] a) S. Kumar, C.-C. An, S. Sahoo, R. Griniene, D. Volyniuk, J. V. Grazulevicius, S. Grigalevicius, J.-H. Jou, *J. Mater. Chem. C* **2017**, *5*, 9854; b) M. Más-Montoya, J. P. Cerón-Carrasco, S. Hamao, R. Eguchi, Y. Kubozono, A. Tárraga, D. Curiel, *J. Mater. Chem. C* **2017**, *5*, 7020; c) Y. Luo, S. Li, Y. Zhao, C. Li, Z. Pang, Y. Huang, M. Yang, L. Zhou, X. Zheng, X. Pu, Z. Lu, *Adv. Mater.* **2020**, *32*, 2001248.
- [8] a) F. Zhang, C. Yi, P. Wei, X. Bi, J. Luo, G. Jacopin, S. Wang, X. Li, Y. Xiao, S. M. Zakeeruddin, M. Grätzel, *Adv. Energy Mater.* **2016**, *6*, 1600401; b) A. Magomedov, S. Paek, P. Gratia, E. Kasparavicius, M. Daskeviciene, E. Kamarauskas, A. Gruodis, V. Jankauskas, K. Kantminiene, K. T. Cho, K. Rakstys, T. Malinauskas, V. Getautis, M. K. Nazeeruddin, *Adv. Funct. Mater.* **2018**, *28*, 1704351;

- c) C. Rodríguez-Seco, M. Méndez, C. Roldán-Carmona, R. Pudi, M. K. Nazeeruddin, E. J. Palomares, *Angew. Chem., Int. Ed.* **2020**, 59, 5303.
- [9] a) N. A. Sayresmith, A. Saminathan, J. K. Sailer, S. M. Patberg, K. Sandor, Y. Krishnan, M. G. Walter, *J. Am. Chem. Soc.* **2019**, 141, 18780; b) S. Hu, J. Zeng, X. Zhu, J. Guo, S. Chen, Z. Zhao, B. Z. Tang, *ACS Appl. Mater. Interfaces* **2019**, 11, 27134.
- [10] a) H. Wang, Y. Wen, X. Yang, Y. Wang, W. Zhou, S. Zhang, X. Zhan, Y. Liu, Z. Shuai, D. Zhu, *ACS Appl. Mater. Interfaces* **2009**, 1, 1122; b) N. P. Liyanage, A. Yella, M. Nazeeruddin, M. Grätzel, J. H. Delcamp, *ACS Appl. Mater. Interfaces* **2016**, 8, 5376; c) M. B. Desta, N. S. Vinh, C. P. Kumar, S. Chaurasia, W.-T. Wu, J. T. Lin, T.-C. Wei, E. W.-G. Diau, *J. Mater. Chem. A* **2018**, 6, 13778.
- [11] a) T.-A. Lin, T. Chatterjee, W.-L. Tsai, W.-K. Lee, M.-J. Wu, M. Jiao, K.-C. Pan, C.-L. Yi, C.-L. Chung, K.-T. Wong, C.-C. Wu, *Adv. Mater.* **2016**, 28, 6976; b) L. Gan, Z. Xu, Z. Wang, B. Li, W. Li, X. Cai, K. Liu, Q. Liang, S.-J. Su, *Adv. Funct. Mater.* **2019**, 29, 1808088; c) S.-J. Woo, Y. Kim, S.-K. Kwon, Y.-H. Kim, J.-J. Kim, *ACS Appl. Mater. Interfaces* **2019**, 11, 7199.
- [12] a) C. Chen, C. Fang, *Chem. Asian J* **2020**, 15, 1514; b) H. Zhang, A. Li, G. Li, B. Li, Z. Wang, S. Xu, W. Xu, B. Z. Tang, *Adv. Optical Mater.* **2020**, 8, 1902195.
- [13] S. Ye, C. Wu, P. Gu, T. Xiang, S. Zhang, T. Jing, S. Wang, X. Yang, Y. Li, W. Huang, *J. Mater. Chem. C* **2020**, 8, 16870.
- [14] P. Meti, H.-H. Park, Y.-D. Gong, *J. Mater. Chem. C* **2020**, 8, 352.
- [15] T. Huang, D. Liu, J. Jiang, W. Jiang, *Chem. Eur. J.* **2019**, 25, 10926.
- [16] C.-C. Huang, M.-M. Xue, F.-P. Wu, Y. Yuan, L.-S. Liao, M.-K. Fung, *Molecules* **2019**, 24, 353.
- [17] L. Wei, J. Li, K. Xue, S. Ye, H. Jiang, *New J. Chem.* **2019**, 43, 16629.
- [18] a) M. Chen, H. Nie, B. Song, L. Li, J. Z. Sun, A. Qin, B. Z. Tang, *J. Mater. Chem. C* **2016**, 4, 2901; b) L. Pan, H. Wu, J. Liu, K. Xue, W. Luo, P. Chen, Z. Wang, A. Qin, B. Z. Tang, *Adv. Optical Mater.* **2019**, 7, 1801673; c) H. Wu, Y. Pan, J. Zeng, L. Du, W. Luo, H. Zhang, K. Xue, P. Chen, D. L. Phillips, Z. Wang, A. Qin, B. Z. Tang, *Adv. Optical Mater.* **2019**, 7, 1900283; d) H. Wu, J. Luo, Z. Xu, Z. Wang, D. Ma, A. Qin, B. Z. Tang, *Chem. Res. Chinese Univ.* **2020**, 36, 61.
- [19] H. Wu, J. Zeng, Z. Xu, B. Zhang, H. Zhang, Y. Pan, Z. Wang, D. Ma, A. Qin, B. Z. Tang, *J. Mater. Chem. C* **2019**, 7, 13047.
- [20] H. Wu, X. Song, B. Zhang, Z. Wang, T. Zhang, A. Qin, B. Z. Tang, *Mater. Chem. Front.* **2020**, 4, 1706.
- [21] Q. Li, Z. Li, *Acc. Chem. Res.* **2020**, 53, 962.
- [22] a) Q. Wu, T. Zhang, Q. Peng, D. Wang, Z. Shuai, *Phys. Chem. Chem. Phys.* **2014**, 16, 5545; b) F. Bu, R. Duan, Y. Xie, Y. Yi, Q. Peng, R. Hu, A. Qin, Z. Zhao, B. Z. Tang, *Angew. Chem., Int. Ed.* **2015**, 54, 14492.
- [23] a) T. Lu, F. Chen, *J. Comput. Chem.* **2012**, 33, 580; b) S. Mukhopadhyay, S. P. Jagtap, V. Coropceanu, J.-L. Brédas, D. M. Collard, *Angew. Chem., Int. Ed.* **2012**, 51, 11629; c) S. Biswas, A. Pramanik, S. Pal, P. Sarkar, *J. Phys. Chem. C* **2017**, 121, 2574.